

## Comparison of DC-DC converters for solar power conversion system

Debani Prasad Mishra<sup>1</sup>, Rudranarayan Senapati<sup>2</sup>, Surender Reddy Salkuti<sup>3</sup>

<sup>1</sup>Department of Electrical Engineering, IIIT Bhubaneswar, Bhubaneswar, India

<sup>2</sup>Department Electrical Engineering, KIIT Deemed to be University, Bhubaneswar, India

<sup>3</sup>Department of Railroad and Electrical Engineering, Woosong University, Daejeon, Republic of Korea

### Article Info

#### Article history:

Received Jul 21, 2021

Revised Mar 9, 2022

Accepted Mar 15, 2022

#### Keywords:

DC-DC power converters

MPPT algorithm

Non-inverting buck-boost

Photovoltaic systems

PV panel

### ABSTRACT

This paper covers the comparison between four different DC-DC converters for solar power conversion. The four converters are buck converter, buck-boost converter, boost converter, and noninverting buck-boost converter. An maximum power point tracking (MPPT) algorithm is designed to calculate battery voltage, current of photovoltaic (PV) array, the voltage of PV array, power of PV array, output power. It is observed that the non-inverting buck-boost converter is the finest converter for solar power conversion. The final circuit design has the results of 12.2 V battery voltage, 0.31 A current of PV array, 34 V voltage of PV array, 23 mW power of PV panel, and 21.8 mW of output power. The efficiency of this system is nearly 95%. All four circuits are simulated in MATLAB/Simulink R2020b.

This is an open access article under the [CC BY-SA](https://creativecommons.org/licenses/by-sa/4.0/) license.



### Corresponding Author:

Surender Reddy Salkuti

Department of Railroad and Electrical Engineering, Woosong University

17-2, Jayang-Dong, Dong-Gu, Daejeon-34606, Republic of Korea

Email: surender@wsu.ac.kr

## 1. INTRODUCTION

The world has a keen interest in collecting knowledge about the earth, its neighboring planets, and moons of different planets, the sun, and also different galaxies. This all can be possibly done by space exploration. NASA has done some phenomenal work on nuclear power systems [1]. Space exploration is done by satellites that need electrical power to do their required work [2]. In recent years there have been several satellites launched in space for scientific research [3], mobile communication, remote sensing, mapping of an area, navigation of ships, vehicles, planes, and drones. In space, satellites need electrical power which can only be provided by solar energy. Tennakoon *et al.* [4], there is an explanation about maximizing solar energy uses. Satellites need to convert solar energy to electrical energy and need to store energy to do their required work. Mars Rover is one of the examples of this process [5]. Some evolutionary computing techniques were also used to reduce the cost of satellites or other spacecraft [6]. The electric power system is explained in reference [7]. In the energy conversion process from solar to electric, DC microgrid and DC-DC converters come into play. Some research was also done for DC-microgrids for space application [8]. D'Antonio *et al.* [9], some mathematical approach was used to decrease the overall mass of the power system used in space exploration. Baharudin *et al.* [10] a photovoltaic (PV) power system is presented which is of high efficiency and has a very compact design. Several types of DC-DC converters can be used in solar power conversion microgrids [11].

A microgrid is a local energy grid that is self-sufficient and has control over itself. It can connect and disconnect from the main grid and can operate on its own. Renewable resources like wind energy, solar

panels can be used to power microgrids. It has many advantages including better power quality and being more environment friendly [12]. A microgrid can be constructed to run indefinitely if we know how it's fueled and how efficiently we can manage its requirements. Energy management strategies are used for maximum optimization of microgrids [13]. The isolation technology of microgrids makes it more reliable [14]. DC-DC converters are the circuits that are used to convert one dc voltage into another dc voltage. This converter can be used in very low voltage as well as very high voltage applications. These converters can boost solar energy up to 30% in solar applications. This type of converter can provide different voltages to different components of a system to gain maximum output from that system or to increase the overall performance of the system. It reduces conduction losses with optimum peak current to increase efficiency to maximum [15].

The solar microgrid can be designed by using maximum power point tracking (MPPT) technology. In this technology, PV panels relate to the DC-DC converter, and it is further connected to load or some energy storage device, and the MPPT controller is connected in parallel to the PV panels and series with the DC-DC converter. This method brings highly reliable, maintenance-free, and highly flexible operation to the system [16]. The MPPT controller is based on the MPPT algorithm [17]. This algorithm is applied in photovoltaic systems. The degree of sunlight falling on the PV panel (solar irradiance) always changes throughout the day, the tracker finds the sweet spot on the PV panel where the current and voltage is maximum. There are different MPPT algorithms, but the perturb and observe algorithm (P&O) method is the simplest [18]. The circuits of DC-DC converters are designed in MATLAB/Simulink and the MPPT algorithm is implemented for obtaining power from each converter. The efficiency graph obtained from Simulink is compared. The P&O method is used since it is reliable, and its hardware implementation is also simple.

**2. RESEARCH METHOD**

**2.1. Variable identification**

In this research, to proceed further and apply the MPPT algorithm. The following variables need to be identified: PV voltage ( $v_{PV}$ ), PV current ( $i_{PV}$ ), PV power ( $p_{PV}$ ), output current ( $I_{out}$ ), output voltage or battery voltage ( $V_{out}$ ), and output power ( $P_{out}$ ). The  $v_{PV}$  and  $i_{PV}$  can also be referred to as input voltage and input current respectively for DC-DC converters.

**2.2. MPPT algorithm**

The P&O method of the MPPT algorithm is used [19], [20] since there is no complex computation, and its hardware implementation is also simple. Some papers research the evaluation of the P&O method [21], [22]. There are other methods to optimize the system like the MPSO method based on the MPPT algorithm [23]. The MPPT function block where MPPT code is written is shown in Figure 1. The P&O method is explained in the flowchart given in Figure 2.

Figure 1 depicts the MPPT function block and pulse width modulation (PWM) generator block. The MPPT function is written for the MPPT block and  $v_{PV}$  and  $i_{PV}$  is given as input and duty is taken out as output. Further, the duty output is the input for the PWM generator and PWM is coming out as output is further transferred to the MOSFET of the converter [24], [25]. Figure 2 depicts the flowchart of the algorithm used in the MPPT function. The algorithm starts by reading  $v_{PV}$  and  $i_{PV}$  from solar panels and setting the maximum power to initial value (usually zero). Then we need old and new values of voltage and power to calculate the difference between them because this algorithm searches for derivatives of power with respect to voltage (i.e.  $dP/dV$ ). Then it checks If  $dP/dV = 0$  duty will not change and if the old value power is not equal to the new value of power and PV voltage greater than 30 V then the algorithm will work, and the final duty will be computed.

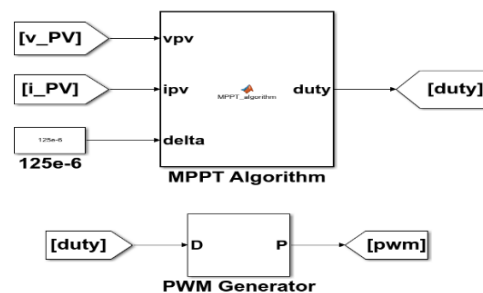


Figure 1. MPPT function and PWM generator

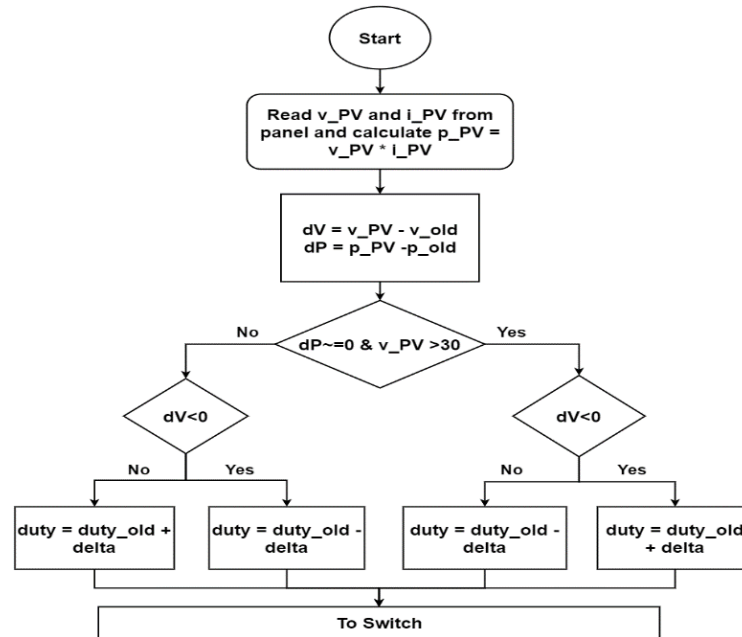


Figure 2. Flowchart of P&O Method of MPPT algorithm

### 2.3. Circuit design and simulation

The circuit is designed in MATLAB/Simulink. The PV modules integrated with DC-DC converters are classified into two groups: full power and partial power conversion and full power conversion [26]. The DC-DC converters can be cascaded with PV modules [27]. Some connections problems arise due to cascading DC-DC converters whose solution can be found in reference [28]. When DC-DC converters are added on the PV module level there is a large amount of power dropped off the whole PV system [29]. The circuit diagrams of buck, boost, and buck-boost is stated in [30]–[32]. Narasimha and Salkuti [33], a detailed analysis of the buck-boost converter is presented. The PV panel, DC-DC converter, and load are connected in series. The output coming out of the MPPT function is given to the PWM generator and the output coming out of it is given to the metal oxide semiconductor field effect transistor (MOSFET) of the converter in Figure 1. Different combinations of resistance, capacitor, and inductor are used to obtain maximum efficiency from each converter. Figure 3 depicts buck topology, Figure 4 depicts boost topology, Figure 5 depicts buck-boost topology, and Figure 6 depicts non-inverting buck-boost topology. The values of resistance, capacitor, and inductor are shown in Figures 3-6 of each circuit diagram. The values of capacitor and inductor for non-inverting buck-boost are  $C_i = 4 \mu F$ ,  $L = 122 \mu H$ ,  $C_o = 7 \mu F$ .

Figure 3 depicts the circuit of the buck converter. The irradiance curve and temperature are given as the input to the PV array block. The PV array block is cascaded with a buck converter and load. After simulation,  $V_{out}$  and  $I_{out}$  are obtained from using a scope. It is known that the product of voltage and current gives power. Then output current and output voltage are simulated through a multiplier and power is obtained similarly the power of a PV panel is obtained by multiplying  $i_{PV}$  and  $v_{PV}$ . The obtained value of  $v_{PV} = 33.9$  V,  $i_{PV} = 0.239$  A,  $V_{out} = 9.6$  V,  $I_{out} = 0.48$  A,  $p_{PV} = 0.012$  W,  $P_{out} = 0.0112$  W,  $C_i = 100 \mu F$ ,  $L = 783 \mu H$ ,  $C_o = 36400 \mu F$ .

Figure 4 depicts the circuit of the boost converter. The irradiance curve and temperature are given as the input to the PV array block. Then the PV array block is cascaded with a boost converter and load. After simulation,  $V_{out}$  and  $I_{out}$  are obtained from using a scope. It is known that the product of voltage and current gives power. Then output current and output voltage are simulated through a multiplier and power is obtained similarly the power of a PV panel is obtained by multiplying  $i_{PV}$  and  $v_{PV}$ . The obtained value of  $v_{PV} = 4.37$  V,  $i_{PV} = 0.258$  A,  $V_{out} = 4.37$  V,  $I_{out} = 0.0027$  A,  $p_{PV} = 0.0031$  W,  $P_{out} = 0.0027$  W,  $C_i = 100 \mu F$ ,  $L = 0.002 \mu H$ ,  $C_o = 100 \mu F$ .

Figure 5 depicts the buck-boost converter circuit. The irradiance curve and temperature are given as the input to the PV array block. Then the PV array block is cascaded with a buck-boost converter and load. After simulation,  $V_{out}$  and  $I_{out}$  are obtained from using a scope. It is known that the product of voltage and current gives power. Then output current and output voltage are simulated through a multiplier and power is obtained similarly the power of a PV panel is obtained by multiplying  $i_{PV}$  and  $v_{PV}$ . The obtained value of

$v_{PV} = 5.6 \text{ V}$ ,  $i_{PV} = 0.25 \text{ A}$ ,  $V_{out} = 4.7 \text{ V}$ ,  $I_{out} = 0.23 \text{ A}$ ,  $p_{PV} = 0.00406 \text{ W}$ ,  $P_{out} = 0.0032 \text{ W}$ ,  $C_i = 100 \mu\text{F}$ ,  $L = 783 \mu\text{H}$ ,  $C_o = 100 \mu\text{F}$ .

Figure 6 depicts the circuit of a noninverting buck-boost converter. The irradiance curve and temperature are given as the input to the PV array block. Then the PV array block is cascaded with a noninverting buck-boost converter and load. After simulation,  $V_{out}$  and  $I_{out}$  are obtained from using a scope. It is known that the product of voltage and current gives power. Then output current and output voltage are simulated through a multiplier and power is obtained similarly the power of a PV panel is obtained by multiplying  $v_{PV}$  and  $i_{PV}$ . The obtained value of  $v_{PV} = 34 \text{ V}$ ,  $i_{PV} = 0.31 \text{ A}$ ,  $V_{out} = 12.2 \text{ V}$ ,  $I_{out} = 0.61 \text{ A}$ ,  $p_{PV} = 0.02302 \text{ W}$ ,  $P_{out} = 0.02185 \text{ W}$ ,  $C_i = 4 \mu\text{F}$ ,  $L = 122 \mu\text{H}$ ,  $C_o = 7 \mu\text{F}$ .

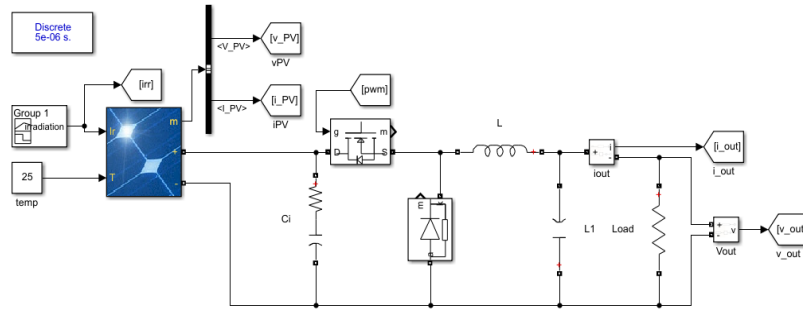


Figure 3. Buck topology

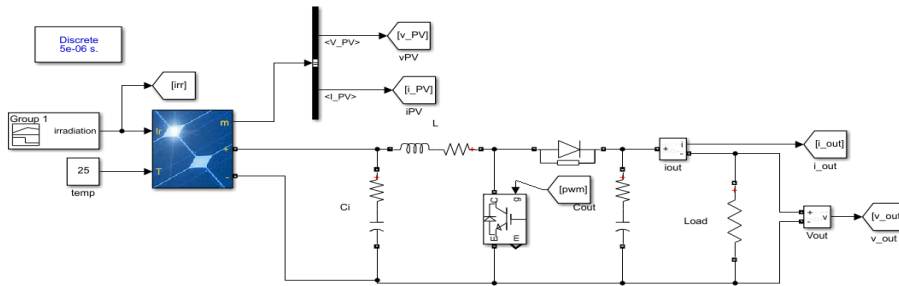


Figure 4. Boost topology

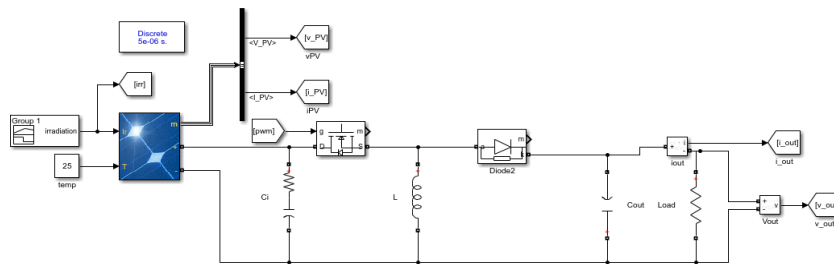


Figure 5. Buck-boost topology

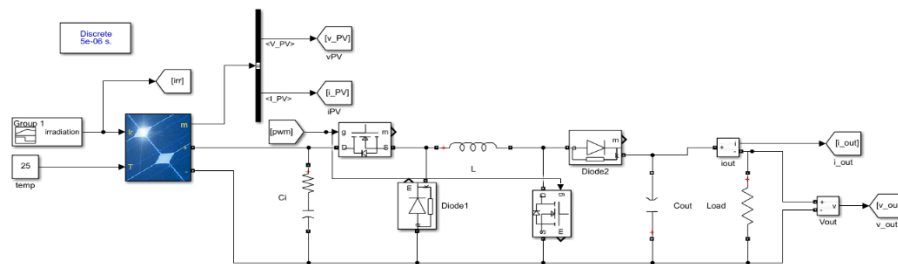


Figure 6. Noninverting buck-boost topology

### 3. RESULT AND DISCUSSION

The circuits are simulated for 0.6 seconds in MATLAB/Simulink. The values of each variable are calculated from the graphs of each variable. The root mean square (RMS) value is calculated from each graph. The graph of efficiency is also obtained by using this formula of efficiency in MATLAB/Simulink i.e. ( $\text{eff} = (\text{Pout}/\text{Pin}) * 100$ ). The results obtained from the simulation are presented in Table 1.

Table 1. Values of variables

Variable	Buck	Boost	Buck-Boost	NIBB
$V_{out}$ [V]	9.6	4.37	4.7	12.2
$p_{PV}$ [W]	0.012	0.0031	0.0032	0.023
$v_{PV}$ [V]	33.9	4.37	5.6	34
$P_{out}$ [W]	0.0112	0.0027	0.0032	0.02185
$i_{PV}$ [A]	0.239	0.258	0.25	0.31
$I_{out}$ [A]	0.48	0.0027	0.23	0.61

Table 1 shows the value of parameters or variables. These values are calculated from a graph of each variable. First, the scope block is used in Simulink to obtain the graph then we used the signal statistic tool to get the root mean square value of the given graph. The graph of each variable is obtained by simulating the circuits in MATLAB/Simulink. Using the values of variables, efficiency is calculated. After the simulation the values of input current, input voltage are taken and given to multiplier to calculate input power, and similarly, the output power is calculated then from using a scope, graphs of both the power are obtained from which we have computed the RMS value of both input and output power. By taking the ratio of output power and input power, efficiency is calculated.

#### 3.1. Efficiency

The graph of Pin/Pout ratio vs time graph of four different converters is obtained by using the Maximum point tracking algorithm in MATLAB/Simulink. The formula used for calculating efficiency is  $P_{out}/p_{PV} * 100\%$ . In Figure 7, for the boost converter, the efficiency is nearly 87%. In Figure 8, it can be seen that the buck converter efficiency is nearly 93%. In Figure 9 we can see that the buck-boost converter efficiency is nearly 78%. From Figure 10, it can be observed that the efficiency of noninverting buck-boost converters is nearly 95%.

Figure 7 depicts the efficiency vs time curve of the boost converter. The x-axis is efficiency (ratio of output and input power) and the y-axis is for the time in seconds. It can be seen from the graph that it initially starts from zero and goes upto 0.5 in a short interval of time then it remains nearly constant upto 0.45 seconds and then goes upto 0.9 at 0.6 seconds. When the RMS value of the graph is calculated using Simulink it comes out to be 0.56. When the efficiency of the boost converter is calculated from the formula  $(\text{Pout}/\text{Pin} * 100)$ , it comes out to be nearly 87%.

Figure 8 depicts the efficiency vs time curve of boost topology. The x-axis is of efficiency (ratio of output and input power) and the y-axis is for the time in seconds. It can be seen from the graph that it initially starts from zero and goes upto 0.5 in the short interval of time then it remains nearly constant upto 0.4 seconds then it falls to 0.1 in a very short period of time and then goes upto 0.8 at 0.6 seconds. When the RMS value of the graph is calculated using Simulink it comes out to be 0.0032. When the efficiency of the buck-boost converter is calculated from the formula  $(\text{Pout}/\text{Pin} * 100)$ , it comes out to be nearly 78%.

Figure 9 depicts the efficiency vs time curve of buck topology. The x-axis is efficiency (ratio of output and input power) and the y-axis is for the time in seconds. This graph fluctuates very fast. It starts from zero then it reaches upto 0.7 in 0.35 seconds then comes down to 0 at 0.3 seconds then it reaches 0.9 at 0.35 seconds then again it comes down to zero in a very short period and then it fluctuated more between 0 and 0.9 and finally get saturated near 0.9 at 0.6 seconds. When the RMS value of the graph is calculated using Simulink it comes out to be 3.4. When the efficiency of the buck topology is calculated from the formula  $(\text{Pout}/\text{Pin} * 100)$ , it comes out to be nearly 93%.

Figure 10 depicts the efficiency vs time curve of a non-inverting buck-boost converter. The x-axis is efficiency (ratio of output and input power) and the y-axis is for the time in seconds. The signal in this graph fluctuates more than the buck topology. It starts from 0 then goes upto 0.5 in 0.1 seconds and reach zero in a very short period of time then goes upto 0.6 remains constant for a short period of time then comes to 0.1 in 0.25 seconds and goes above 1.6 in a very short period of time then after oscillating comes down to 0.7 in 0.35 seconds then it fluctuates between zero and 1.6 for more 0.1 seconds and get saturated at 0.95. When the RMS value of the graph is calculated using Simulink it comes out to be 4.3. When the efficiency of the non-inverting buck-boost topology is calculated from the formula  $(\text{Pout}/\text{Pin} * 100)$ , it comes out to be nearly 95%.

After simulating each circuit in MATLAB/Simulink, the RMS value of the graph (efficiency vs time) is observed. The RMS value can be acquired by using the signal statistic tool present in the Simulink. The RMS values obtained are 3.4 for the buck converter, 0.56 for the boost converter, 0.0032 for the buck-boost converter, and 4.3 for the non-inverting buck-boost converter. From these results, we can also say that the non-inverting buck-boost converter has the highest RMS value so it is most efficient.

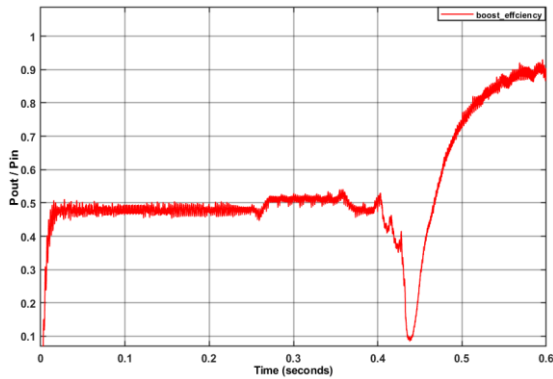


Figure 7. Boost topology efficiency

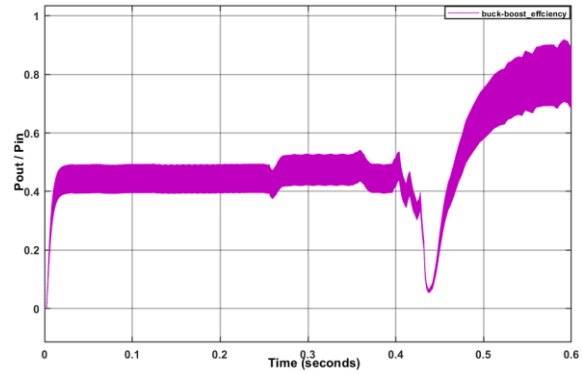


Figure 8. Buck-boost topology efficiency

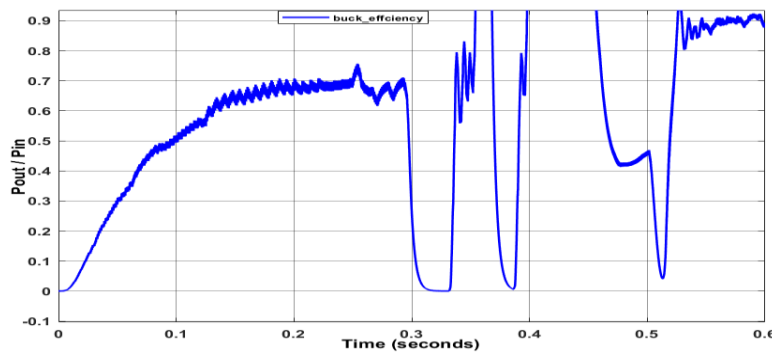


Figure 9. Buck topology efficiency

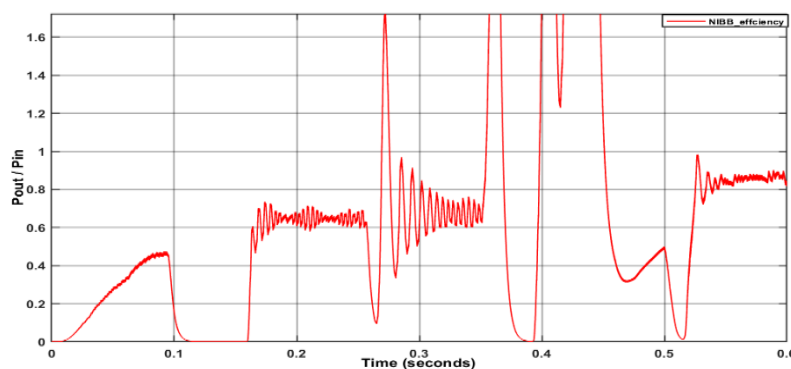


Figure 10. Non-inverting buck-boost topology efficiency

#### 4. CONCLUSION

This paper presents the comparison of the efficiency of four converters i.e. boost, buck-boost, buck, and non-inverting buck-boost converters. An MPPT algorithm is designed which uses the P&O method to maximize the output power and to obtain maximum efficiency. All the circuits are designed in MATLAB/Simulink and each circuit is simulated to obtain a graph of the efficiency of each converter. The values of variables are calculated using simulation results. The efficiency of each converter is calculated and

compared. The result is that the non-inverting buck-boost converter shows a maximum efficiency of nearly 95%. After all the analysis, the system parameters were 12.2 V load voltage or battery voltage, 0.31 A current of PV array, 34 V voltage of PV array, 23 mW power of PV array, and 21.8 mW of output power.

## ACKNOWLEDGEMENTS

This research work was funded by “Woosong University’s Academic Research Funding - 2022”.




## REFERENCES

- [1] T. S. Balint, “Nuclear systems for Mars exploration,” in *2004 IEEE Aerospace Conference Proceedings (IEEE Cat. No.04TH8720)*, 2004, pp. 2958–2977, doi: 10.1109/AERO.2004.1368102.
- [2] N. A. Ja’ and M. A. Watson, “Benchmarking the human exploration of Mars design reference architecture,” *International Journal of Space Science and Engineering*, vol. 5, no. 2, p. 138, 2019, doi: 10.1504/IJSPACESE.2019.097410.
- [3] I. Bisio, R. De Gaudenzi, H. Nguyen, F.-N. Pavlidou, and T. Yamazato, “Recent advances in satellite and space communications,” *Journal of Communications and Networks*, vol. 12, no. 6, pp. 523–528, Dec. 2010, doi: 10.1109/JCN.2010.6388298.
- [4] S. M. Tennakoon, W. W. L. Keerthipala, and W. B. Lawrance, “Solar energy for development of a cost-effective building energy system,” in *PowerCon 2000. 2000 International Conference on Power System Technology. Proceedings (Cat. No.00EX409)*, vol. 1, 2002, pp. 55–59, doi: 10.1109/ICPST.2000.900031.
- [5] J. Dongsheng and Z. Pei, “An electrical power system of Mars rover,” in *2014 IEEE Conference and Expo Transportation Electrification Asia-Pacific (ITEC Asia-Pacific)*, Aug. 2014, pp. 1–4, doi: 10.1109/ITEC-AP.2014.6940651.
- [6] R. J. Terrile, M. Kordon, D. Mandutianu, J. Salcedo, E. Wood, and M. Hashemi, “Automated design of spacecraft power subsystems,” in *2006 IEEE Aerospace Conference*, 2006, pp. 1–14, doi: 10.1109/AERO.2006.1656181.
- [7] E. B. Gietl, E. W. Gholdston, B. A. Manners, and R. A. Delventhal, “The electric power system of the international space station—a platform for power technology development,” in *2000 IEEE Aerospace Conference. Proceedings (Cat. No.00TH8484)*, vol. 4, 2000, pp. 47–54, doi: 10.1109/AERO.2000.878364.
- [8] D. Tan, D. Baxter, S. Foroozan, and S. Crane, “A first resilient DC-dominated microgrid for mission-critical space applications,” *IEEE Journal of Emerging and Selected Topics in Power Electronics*, vol. 4, no. 4, pp. 1147–1157, Dec. 2016, doi: 10.1109/JESTPE.2016.2615763.
- [9] M. D’Antonio, C. Shi, B. Wu, and A. Khaligh, “Design and optimization of a solar power conversion system for space applications,” *IEEE Transactions on Industry Applications*, vol. 55, no. 3, pp. 2310–2319, May 2019, doi: 10.1109/TIA.2019.2891228.
- [10] N. H. Baharudin, T. M. N. T. Mansur, F. A. Hamid, R. Ali, and M. I. Misrun, “Topologies of DC-DC converter in solar PV applications,” *Indonesian Journal of Electrical Engineering and Computer Science*, vol. 8, no. 2, p. 368, Nov. 2017, doi: 10.11591/ijeecs.v8.i2.pp368-374.
- [11] A. M. Al-Modaffer, A. A. Chlaihawi, and H. A. Wahhab, “Non-isolated multiple input multilevel output DC-DC converter for hybrid power system,” *Indonesian Journal of Electrical Engineering and Computer Science*, vol. 19, no. 2, p. 635, Aug. 2020, doi: 10.11591/ijeecs.v19.i2.pp635-643.
- [12] N. Karthik, A. K. Parvathy, and R. Arul, “A review of optimal operation of microgrids,” *International Journal of Electrical and Computer Engineering (IJECE)*, vol. 10, no. 3, p. 2842, Jun. 2020, doi: 10.11591/ijece.v10i3.pp2842-2849.
- [13] M. R. B. Khan, J. Pasupuleti, J. Al-Fattah, and M. Tahmasebi, “Energy management system for PV-battery microgrid based on model predictive control,” *Indonesian Journal of Electrical Engineering and Computer Science*, vol. 15, no. 1, p. 20, Jul. 2019, doi: 10.11591/ijeecs.v15.i1.pp20-26.
- [14] B. Kroposki, T. Basso, and R. DeBlasio, “Microgrid standards and technologies,” in *2008 IEEE Power and Energy Society General Meeting - Conversion and Delivery of Electrical Energy in the 21st Century*, Jul. 2008, pp. 1–4, doi: 10.1109/PES.2008.4596703.
- [15] B. Arbetter, R. Erickson, and D. Maksimovic, “DC-DC converter design for battery-operated systems,” in *Proceedings of PESC ’95 - Power Electronics Specialist Conference*, vol. 1, 1995, pp. 103–109, doi: 10.1109/PESC.1995.474799.
- [16] B. Mohammed, B. Kadri, N. Abdelfatah, and B. Ismail, “Design and modeling of optical reflectors for a PV panel adapted by MPPT control,” *Indonesian Journal of Electrical Engineering and Computer Science*, vol. 16, no. 2, p. 653, Nov. 2019, doi: 10.11591/ijeecs.v16.i2.pp653-660.
- [17] F. R. Islam, K. Prakash, K. A. Mamun, A. Lallu, and R. Mudliar, “Design a optimum MPPT controller for solar energy system,” *Indonesian Journal of Electrical Engineering and Computer Science*, vol. 2, no. 3, p. 545, Jun. 2016, doi: 10.11591/ijeecs.v2.i3.pp545-553.
- [18] J. Ahmed and Z. Salam, “An improved perturb and observe (P&O) maximum power point tracking (MPPT) algorithm for higher efficiency,” *Applied Energy*, vol. 150, pp. 97–108, Jul. 2015, doi: 10.1016/j.apenergy.2015.04.006.
- [19] H. M. A. Alhussain and N. Yasin, “Modeling and simulation of solar PV module for comparison of two MPPT algorithms (P&O & INC) in MATLAB/Simulink,” *Indonesian Journal of Electrical Engineering and Computer Science*, vol. 18, no. 2, p. 666, May 2020, doi: 10.11591/ijeecs.v18.i2.pp666-677.
- [20] M. A. Elgendy, B. Zahawi, and D. J. Atkinson, “Evaluation of perturb and observe MPPT algorithm implementation techniques,” in *6th IET International Conference on Power Electronics, Machines and Drives (PEMD 2012)*, 2012, pp. P110–P110, doi: 10.1049/cp.2012.0156.
- [21] K. P. Panda, A. Anand, P. R. Bana, and G. Panda, “Novel PWM control with modified PSO-MPPT algorithm for reduced switch MLI based standalone PV system,” *International Journal of Emerging Electric Power Systems*, vol. 19, no. 5, Oct. 2018, doi: 10.1515/ijeeps-2018-0023.
- [22] M. Kasper, D. Bortis, and J. W. Kolar, “Classification and comparative evaluation of PV panel-integrated DC-DC converter concepts,” *IEEE Transactions on Power Electronics*, vol. 29, no. 5, pp. 2511–2526, May 2014, doi: 10.1109/TPEL.2013.2273399.
- [23] A. I. Bratcu, I. Munteanu, S. Bacha, D. Picault, and B. Raison, “Cascaded DC-DC converter photovoltaic systems: power optimization issues,” *IEEE Transactions on Industrial Electronics*, vol. 58, no. 2, pp. 403–411, Feb. 2011, doi: 10.1109/TIE.2010.2043041.




- [24] R. Kadri, J.-P. Gaubert, and G. Champenois, "Nondissipative string current diverter for solving the cascaded DC-DC converter connection problem in photovoltaic power generation system," *IEEE Transactions on Power Electronics*, vol. 27, no. 3, pp. 1249–1258, Mar. 2012, doi: 10.1109/TPEL.2011.2164268.
- [25] H. J. Bergveld *et al.*, "Module-level DC/DC conversion for photovoltaic systems: the delta-conversion concept," *IEEE Transactions on Power Electronics*, vol. 28, no. 4, pp. 2005–2013, Apr. 2013, doi: 10.1109/TPEL.2012.2195331.
- [26] Y. H. Lho and S. R. Salkuti, "A Study on TID and SEL tests on PWM-IC controller of DC/DC power buck converter," *International Journal of Control and Automation*, vol. 10, no. 6, pp. 137–148, Jun. 2017, doi: 10.14257/ijca.2017.10.6.14.
- [27] H. Bai, C. Mi, C. Wang, and S. Gargies, "The dynamic model and hybrid phase-shift control of a dual-active-bridge converter," in *2008 34th Annual Conference of IEEE Industrial Electronics*, Nov. 2008, pp. 2840–2845, doi: 10.1109/IECON.2008.4758409.
- [28] M. F. Omar and H. C. M. Haris, "Series-loaded resonant converter DC-DC buck operating for low power," *Indonesian Journal of Electrical Engineering and Computer Science*, vol. 8, no. 1, p. 159, Oct. 2017, doi: 10.11591/ijeecs.v8.i1.pp159-168.
- [29] P. Nandi and R. Adda, "Integration of boost-type active power decoupling topology with single-phase switched boost inverter," *IEEE Transactions on Power Electronics*, vol. 35, no. 11, pp. 11965–11975, Nov. 2020, doi: 10.1109/TPEL.2020.2988402.
- [30] A. Kalirasu, "A novel single source multiple output converter integrating buck-boost and fly back topology for SMPS applications," *Indonesian Journal of Electrical Engineering and Computer Science*, vol. 8, no. 3, p. 733, Dec. 2017, doi: 10.11591/ijeecs.v8.i3.pp733-736.
- [31] S. Narasimha and S. R. Salkuti, "An improved closed loop hybrid phase shift controller for dual active bridge converter," *International Journal of Electrical and Computer Engineering (IJECE)*, vol. 10, no. 2, p. 1169, Apr. 2020, doi: 10.11591/ijece.v10i2.pp1169-1178.
- [32] P. Sanjeevikumar, G. Grandi, P. W. Wheeler, F. Blaabjerg, and J. Loncarski, "A simple MPPT algorithm for novel PV power generation system by high output voltage DC-DC boost converter," in *2015 IEEE 24th International Symposium on Industrial Electronics (ISIE)*, Jun. 2015, pp. 214–220, doi: 10.1109/ISIE.2015.7281471.
- [33] S. Narasimha and S. R. Salkuti, "Design and operation of closed-loop triple-deck buck-boost converter with high gain soft switching," *International Journal of Power Electronics and Drive Systems (IJPEDS)*, vol. 11, no. 1, p. 523, Mar. 2020, doi: 10.11591/ijped.v11.i1.pp523-529.

## BIOGRAPHIES OF AUTHORS






**Debani Prasad Mishra**    received the B.Tech. in electrical engineering from the Biju Patnaik University of Technology, Odisha, India, in 2006 and the M.Tech in power systems from IIT, Delhi, India in 2010. He has been awarded the Ph.D. degree in power systems from Veer Surendra Sai University of Technology, Odisha, India, in 2019. He is currently serving as Assistant Professor in the Dept of Electrical Engg, International Institute of Information Technology Bhubaneswar, Odisha. He has 11 years of teaching experience and 2 years of industry experience in the thermal power plant. He is the author of more than 80 research articles. His research interests include soft Computing techniques application in power system, signal processing and power quality 3 students have been awarded Ph.D under his guidance and currently 4 Ph.D. Scholars are continuing under him. He can be contacted at email: debani@iiit-bh.ac.in.



**Rudranarayan Senapati**    received his B.E. degrees in Electrical Engineering from Indira Gandhi Institute of Technology (IGIT), Sarang, Odisha, India, under Utkal University in 2001 and M.Tech degree in Communication Systems Engineering, from KIIT University in 2006. He has been awarded the Ph.D. degree in power systems from KIIT Deemed to be University, Bhubaneswar, Odisha, India, in 2018. Currently he is working as Assistant Professor in School of Electrical Engineering, KIIT Deemed to be University. He is the author of more than 25 research articles. His current research interests include grid integration of renewable energy sources, PQ conditioners and PQ control and analysis, smart grids and Micro Grids, Blockchain Technology. He can be contacted at email: rsenapatifel@kiit.ac.in.



**Surender Reddy Salkuti**    received the Ph.D. degree in electrical engineering from the Indian Institute of Technology, New Delhi, India, in 2013. He was a Postdoctoral Researcher with Howard University, Washington, DC, USA, from 2013 to 2014. He is currently an Associate Professor with the Department of Railroad and Electrical Engineering, Woosong University, Daejeon, South Korea. His current research interests include power system restructuring issues, ancillary service pricing, real and reactive power pricing, congestion management, and market clearing, including renewable energy sources, demand response, smart grid development with integration of wind and solar photovoltaic energy sources, artificial intelligence applications in power systems, and power system analysis and optimization. He can be contacted at email: surender@wsu.ac.kr.